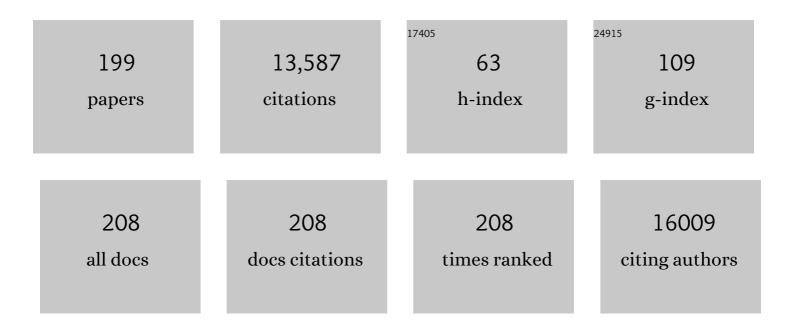


## List of Publications by Year in descending order

Source: https://exaly.com/author-pdf/272975/publications.pdf Version: 2024-02-01



LUAN SU

#	Article	IF	CITATIONS
1	Metal-Free Activation of Dioxygen by Graphene/g-C <sub>3</sub> N <sub>4</sub> Nanocomposites: Functional Dyads for Selective Oxidation of Saturated Hydrocarbons. Journal of the American Chemical Society, 2011, 133, 8074-8077.	6.6	567
2	Janus Co/CoP Nanoparticles as Efficient Mott–Schottky Electrocatalysts for Overall Water Splitting in Wide pH Range. Advanced Energy Materials, 2017, 7, 1602355.	10.2	482
3	Surface and Interface Engineering of Electrode Materials for Lithiumâ€ion Batteries. Advanced Materials, 2015, 27, 527-545.	11.1	426
4	Corrosion engineering towards efficient oxygen evolution electrodes with stable catalytic activity for over 6000 hours. Nature Communications, 2018, 9, 2609.	5.8	389
5	Extended Structures and Physicochemical Properties of Uranyl–Organic Compounds. Accounts of Chemical Research, 2011, 44, 531-540.	7.6	375
6	Activating Cobalt Nanoparticles via the Mott–Schottky Effect in Nitrogen-Rich Carbon Shells for Base-Free Aerobic Oxidation of Alcohols to Esters. Journal of the American Chemical Society, 2017, 139, 811-818.	6.6	351
7	Efficient oxygen evolution electrocatalysis in acid by a perovskite with face-sharing IrO6 octahedral dimers. Nature Communications, 2018, 9, 5236.	5.8	325
8	Synthesis, Structure, and Photoelectronic Effects of a Uraniumâ^'Zincâ^'Organic Coordination Polymer Containing Infinite Metal Oxide Sheets. Journal of the American Chemical Society, 2003, 125, 9266-9267.	6.6	302
9	Electrochemical Reduction of N <sub>2</sub> into NH <sub>3</sub> by Donor–Acceptor Couples of Ni and Au Nanoparticles with a 67.8% Faradaic Efficiency. Journal of the American Chemical Society, 2019, 141, 14976-14980.	6.6	290
10	Macroporous V <sub>2</sub> O <sub>5</sub> â^'BiVO <sub>4</sub> Composites: Effect of Heterojunction on the Behavior of Photogenerated Charges. Journal of Physical Chemistry C, 2011, 115, 8064-8071.	1.5	251
11	Water-Insoluble Ag-U-Organic Assemblies with Photocatalytic Activity. Chemistry - A European Journal, 2005, 11, 2642-2650.	1.7	249
12	Surface Binding of Polypyrrole on Porous Silicon Hollow Nanospheres for Liâ€ <del>l</del> on Battery Anodes with High Structure Stability. Advanced Materials, 2014, 26, 6145-6150.	11.1	244
13	Carbon-Coated V <sub>2</sub> O <sub>5</sub> Nanocrystals as High Performance Cathode Material for Lithium Ion Batteries. Chemistry of Materials, 2011, 23, 5290-5292.	3.2	230
14	2D/2D Heterojunctions for Catalysis. Advanced Science, 2019, 6, 1801702.	5.6	224
15	Efficient oxygen evolution reaction catalyzed by low-density Ni-doped Co3O4 nanomaterials derived from metal-embedded graphitic C3N4. Chemical Communications, 2013, 49, 7522.	2.2	220
16	Preparation, Structures, and Photocatalytic Properties of Three New Uranylâ^'Organic Assembly Compounds. Inorganic Chemistry, 2008, 47, 4844-4853.	1.9	210
17	Highly Efficient Dehydrogenation of Formic Acid over a Palladiumâ€Nanoparticleâ€Based Mott–Schottky Photocatalyst. Angewandte Chemie - International Edition, 2013, 52, 11822-11825.	7.2	210
18	Boosting selective nitrogen reduction to ammonia on electron-deficient copper nanoparticles. Nature Communications, 2019, 10, 4380.	5.8	203

#	Article	IF	CITATIONS
19	Efficient Sunlightâ€Driven Dehydrogenative Coupling of Methane to Ethane over a Zn <sup>+</sup> â€Modified Zeolite. Angewandte Chemie - International Edition, 2011, 50, 8299-8303.	7.2	187
20	MoO <sub>2</sub> /Mo <sub>2</sub> C Heteronanotubes Function as Highâ€Performance Liâ€Ion Battery Electrode. Advanced Functional Materials, 2014, 24, 3399-3404.	7.8	185
21	Vinylene-Bridged Two-Dimensional Covalent Organic Frameworks via Knoevenagel Condensation of Tricyanomesitylene. Journal of the American Chemical Society, 2020, 142, 11893-11900.	6.6	180
22	Encapsulating Palladium Nanoparticles Inside Mesoporous MFI Zeolite Nanocrystals for Shapeâ€6elective Catalysis. Angewandte Chemie - International Edition, 2016, 55, 9178-9182.	7.2	174
23	Strongly Veined Carbon Nanoleaves as a Highly Efficient Metalâ€Free Electrocatalyst. Angewandte Chemie - International Edition, 2014, 53, 6905-6909.	7.2	156
24	Direct conversion of urea into graphitic carbon nitride over mesoporous TiO <sub>2</sub> spheres under mild condition. Chemical Communications, 2011, 47, 1066-1068.	2.2	148
25	Synthesis of Amphiphilic Superparamagnetic Ferrite/Block Copolymer Hollow Submicrospheres. Journal of the American Chemical Society, 2006, 128, 8382-8383.	6.6	141
26	Multifunctional Au–Co@CN Nanocatalyst for Highly Efficient Hydrolysis of Ammonia Borane. ACS Catalysis, 2015, 5, 388-392.	5.5	135
27	Facile Synthesis of Thermal―and Photostable Titania with Paramagnetic Oxygen Vacancies for Visibleâ€Light Photocatalysis. Chemistry - A European Journal, 2013, 19, 2866-2873.	1.7	133
28	Strategies to succeed in improving the lithium-ion storage properties of silicon nanomaterials. Journal of Materials Chemistry A, 2016, 4, 32-50.	5.2	130
29	Schottky Barrier Induced Coupled Interface of Electron-Rich N-Doped Carbon and Electron-Deficient Cu: In-Built Lewis Acid–Base Pairs for Highly Efficient CO <sub>2</sub> Fixation. Journal of the American Chemical Society, 2019, 141, 38-41.	6.6	123
30	Toward Hydrogenâ€Free and Dendriteâ€Free Aqueous Zinc Batteries: Formation of Zincophilic Protective Layer on Zn Anodes. Advanced Science, 2022, 9, e2104866.	5.6	118
31	Ultrathin In <sub>2</sub> O <sub>3</sub> Nanosheets with Uniform Mesopores for Highly Sensitive Nitric Oxide Detection. ACS Applied Materials & Interfaces, 2017, 9, 16335-16342.	4.0	108
32	Self-modification of titanium dioxide materials by Ti <sup>3+</sup> and/or oxygen vacancies: new insights into defect chemistry of metal oxides. RSC Advances, 2014, 4, 13979-13988.	1.7	101
33	Syntheses and photoluminescent properties of two uranyl-containing compounds with extended structures. Polyhedron, 2006, 25, 1359-1366.	1.0	100
34	Porous Titania with Heavily Self-Doped Ti <sup>3+</sup> for Specific Sensing of CO at Room Temperature. Inorganic Chemistry, 2013, 52, 5924-5930.	1.9	100
35	Highly Reversible Zinc Anode Enabled by a Cation-Exchange Coating with Zn-Ion Selective Channels. ACS Nano, 2022, 16, 6906-6915.	7.3	100
36	Anchoring Cobalt Nanocrystals through the Plane of Graphene: Highly Integrated Electrocatalyst for Oxygen Reduction Reaction. Chemistry of Materials, 2015, 27, 544-549.	3.2	95

#	Article	IF	CITATIONS
37	Nitrogen-doped graphene microtubes with opened inner voids: Highly efficient metal-free electrocatalysts for alkaline hydrogen evolution reaction. Nano Research, 2016, 9, 2606-2615.	5.8	92
38	Tuning the Adsorption Energy of Methanol Molecules Along Niâ€Nâ€Doped Carbon Phase Boundaries by the Mott–Schottky Effect for Gasâ€Phase Methanol Dehydrogenation. Angewandte Chemie - International Edition, 2018, 57, 2697-2701.	7.2	91
39	Nitrogen-doped carbon nets with micro/mesoporous structures as electrodes for high-performance supercapacitors. Journal of Materials Chemistry A, 2016, 4, 16698-16705.	5.2	88
40	Oxygen Vacancy Engineering of Co <sub>3</sub> O <sub>4</sub> Nanocrystals through Coupling with Metal Support for Water Oxidation. ChemSusChem, 2017, 10, 2875-2879.	3.6	88
41	Synthesis of Ionic Vinyleneâ€Linked Covalent Organic Frameworks through Quaternizationâ€Activated Knoevenagel Condensation. Angewandte Chemie - International Edition, 2021, 60, 13614-13620.	7.2	87
42	Strategies toward Highâ€Performance Cathode Materials for Lithium–Oxygen Batteries. Small, 2018, 14, e1800078.	5.2	86
43	Boosting the Zn-ion transfer kinetics to stabilize the Zn metal interface for high-performance rechargeable Zn-ion batteries. Journal of Materials Chemistry A, 2021, 9, 16814-16823.	5.2	86
44	MOFs of Uranium and the Actinides. Structure and Bonding, 2014, , 265-295.	1.0	84
45	Lithiation mechanism of hierarchical porous MoO <sub>2</sub> nanotubes fabricated through one-step carbothermal reduction. Journal of Materials Chemistry A, 2014, 2, 80-86.	5.2	84
46	A Composite of Carbonâ€Wrapped Mo <sub>2</sub> C Nanoparticle and Carbon Nanotube Formed Directly on Ni Foam as a Highâ€Performance Binderâ€Free Cathode for Liâ€O <sub>2</sub> Batteries. Advanced Functional Materials, 2016, 26, 8514-8520.	7.8	83
47	Hierarchical carbon nanopapers coupled with ultrathin MoS2 nanosheets: Highly efficient large-area electrodes for hydrogen evolution. Nano Energy, 2015, 15, 335-342.	8.2	81
48	Multistaged discharge constructing heterostructure with enhanced solid-solution behavior for long-life lithium-oxygen batteries. Nature Communications, 2019, 10, 5810.	5.8	80
49	Room-temperature transfer hydrogenation and fast separation of unsaturated compounds over heterogeneous catalysts in an aqueous solution of formic acid. Green Chemistry, 2014, 16, 3746-3751.	4.6	79
50	Neuron-Inspired Design of High-Performance Electrode Materials for Sodium-Ion Batteries. ACS Nano, 2018, 12, 11503-11510.	7.3	79
51	Construction of Three-Dimensional Uranyl-Organic Frameworks with Benzenetricarboxylate Ligands. European Journal of Inorganic Chemistry, 2010, 2010, 3780-3788.	1.0	75
52	A graphene-wrapped silver–porous silicon composite with enhanced electrochemical performance for lithium-ion batteries. Journal of Materials Chemistry A, 2013, 1, 13648.	5.2	74
53	Carbonate decomposition: Low-overpotential Li-CO2 battery based on interlayer-confined monodisperse catalyst. Energy Storage Materials, 2018, 15, 291-298.	9.5	73
54	Formation of Single-Crystalline CuS Nanoplates Vertically Standing on Flat Substrate. Crystal Growth and Design, 2007, 7, 2265-2267.	1.4	72

#	Article	IF	CITATIONS
55	Uranyl pyridine-dicarboxylate compounds with clustered water molecules. Inorganic Chemistry Communication, 2006, 9, 595-598.	1.8	68
56	Enriching Co nanoparticles inside carbon nanofibers via nanoscale assembly of metal–organic complexes for highly efficient hydrogen evolution. Nano Energy, 2016, 22, 79-86.	8.2	68
57	Schottky Barrierâ€Induced Surface Electric Field Boosts Universal Reduction of NO <sub><i>x</i></sub> <sup>â^'</sup> in Water to Ammonia. Angewandte Chemie - International Edition, 2021, 60, 20711-20716.	7.2	68
58	Assembly of a manganese(ii) pyridine-3,4-dicarboxylate polymeric network based on infinite Mn–O–C chains. Dalton Transactions, 2003, , 28-30.	1.6	67
59	Synthesis of uranium oxide nanoparticles and their catalytic performance for benzyl alcohol conversion to benzaldehyde. Journal of Materials Chemistry, 2008, 18, 1146.	6.7	67
60	The First Organo-Templated Cobalt Phosphate with a Zeolite Topology. Inorganic Chemistry, 2000, 39, 1476-1479.	1.9	65
61	Freeâ€Standing Air Cathodes Based on 3D Hierarchically Porous Carbon Membranes: Kinetic Overpotential of Continuous Macropores in Liâ€O <sub>2</sub> Batteries. Angewandte Chemie - International Edition, 2018, 57, 6825-6829.	7.2	65
62	Polarized few-layer g-C3N4 as metal-free electrocatalyst for highly efficient reduction of CO2. Nano Research, 2018, 11, 2450-2459.	5.8	65
63	Electrocatalyst design for aprotic Li–CO <sub>2</sub> batteries. Energy and Environmental Science, 2020, 13, 4717-4737.	15.6	65
64	Lowâ€Overpotential Li–O <sub>2</sub> Batteries Based on TFSI Intercalated Co–Ti Layered Double Oxides. Advanced Functional Materials, 2016, 26, 1365-1374.	7.8	64
65	Li <sub>4</sub> Ti <sub>5</sub> O <sub>12</sub> /TiO <sub>2</sub> Hollow Spheres Composed Nanoflakes with Preferentially Exposed Li <sub>4</sub> Ti <sub>5</sub> O <sub>12</sub> (011) Facets for High-Rate Lithium Ion Batteries. ACS Applied Materials & Interfaces, 2014, 6, 19791-19796.	4.0	63
66	Heteroatomâ€Embedded Approach to Vinyleneâ€Linked Covalent Organic Frameworks with Isoelectronic Structures for Photoredox Catalysis. Angewandte Chemie - International Edition, 2022, 61, .	7.2	63
67	Uniform hierarchical MoO2/carbon spheres with high cycling performance for lithium ion batteries. Journal of Materials Chemistry A, 2013, 1, 12038.	5.2	62
68	Fabrication and Growth Mechanism of Selenium and Tellurium Nanobelts through a Vacuum Vapor Deposition Route. Journal of Physical Chemistry C, 2007, 111, 12926-12932.	1.5	60
69	Synthesis and photocatalytic activity of porous anatase TiO2 microspheres composed of {010}-faceted nanobelts. Dalton Transactions, 2013, 42, 4365.	1.6	60
70	Nitrogen-doped carbon nanotube sponge with embedded Fe/Fe <sub>3</sub> C nanoparticles as binder-free cathodes for high capacity lithium–sulfur batteries. Journal of Materials Chemistry A, 2018, 6, 17473-17480.	5.2	60
71	In situ catalytic growth of large-area multilayered graphene/MoS2 heterostructures. Scientific Reports, 2014, 4, 4673.	1.6	58
72	Constructing holey graphene monoliths via supramolecular assembly: Enriching nitrogen heteroatoms up to the theoretical limit for hydrogen evolution reaction. Nano Energy, 2015, 15, 567-575.	8.2	57

#	Article	IF	CITATIONS
73	Controlled Growth and Photocatalytic Properties of CdS Nanocrystals Implanted in Layered Metal Hydroxide Matrixes. Journal of Physical Chemistry B, 2005, 109, 21602-21607.	1.2	56
74	Synthesis, structure characterization and photocatalytic properties of two new uranyl naphthalene-dicarboxylate coordination polymer compounds. Inorganic Chemistry Communication, 2010, 13, 1542-1547.	1.8	55
75	Atomicâ€5cale Mott–Schottky Heterojunctions of Boron Nitride Monolayer and Graphene as Metalâ€Free Photocatalysts for Artificial Photosynthesis. Advanced Science, 2018, 5, 1800062.	5.6	54
76	Enhanced Electrochemical Performance of Aprotic Li O <sub>2</sub> Batteries with a Rutheniumâ€Complexâ€Based Mobile Catalyst. Angewandte Chemie - International Edition, 2021, 60, 16404-16408.	7.2	53
77	A Green Chemistry of Graphene: Photochemical Reduction towards Monolayer Graphene Sheets and the Role of Water Adlayers. ChemSusChem, 2012, 5, 642-646.	3.6	52
78	Nonâ€Conjugated Dicarboxylate Anode Materials for Electrochemical Cells. Angewandte Chemie - International Edition, 2018, 57, 8865-8870.	7.2	52
79	Heterojunctionâ€Based Electron Donators to Stabilize and Activate Ultrafine Pt Nanoparticles for Efficient Hydrogen Atom Dissociation and Gas Evolution. Angewandte Chemie - International Edition, 2021, 60, 25766-25770.	7.2	52
80	Heterometal Alkoxides as Precursors for the Preparation of Porous Fe– and Mn–TiO <sub>2</sub> Photocatalysts with High Efficiencies. Chemistry - A European Journal, 2008, 14, 11123-11131.	1.7	50
81	Mesoporous titania rods as an anode material for high performance lithium-ion batteries. Journal of Power Sources, 2012, 214, 298-302.	4.0	50
82	Template-directed metal oxides for electrochemical energy storage. Energy Storage Materials, 2016, 3, 1-17.	9.5	50
83	Photoluminescent and photovoltaic properties observed in a zinc borate Zn2(OH)BO3. Journal of Materials Chemistry, 2003, 13, 2227-2233.	6.7	49
84	A uranium–zinc–organic molecular compound containing planar tetranuclear uranyl units. Dalton Transactions, 2003, , 4219-4220.	1.6	49
85	Hierarchical Li4Ti5O12/TiO2 composite tubes with regular structural imperfection for lithium ion storage. Scientific Reports, 2013, 3, 3490.	1.6	49
86	A precursor route to single-crystalline WO3 nanoplates with an uneven surface and enhanced sensing properties. Dalton Transactions, 2012, 41, 9773.	1.6	48
87	Light-induced formation of porous TiO2 with superior electron-storing capacity. Chemical Communications, 2010, 46, 2112.	2.2	46
88	Wrinkled Graphene Monoliths as Superabsorbing Building Blocks for Superhydrophobic and Superhydrophilic Surfaces. Angewandte Chemie - International Edition, 2015, 54, 15165-15169.	7.2	45
89	Toward Lower Overpotential through Improved Electron Transport Property: Hierarchically Porous CoN Nanorods Prepared by Nitridation for Lithium–Oxygen Batteries. Nano Letters, 2016, 16, 5902-5908.	4.5	43
90	Grouping Effect of Single Nickelâ^'N <sub>4</sub> Sites in Nitrogenâ€Doped Carbon Boosts Hydrogen Transfer Coupling of Alcohols and Amines. Angewandte Chemie - International Edition, 2018, 57, 15194-15198.	7.2	43

#	Article	IF	CITATIONS
91	Photochemically Engineering the Metal–Semiconductor Interface for Roomâ€Temperature Transfer Hydrogenation of Nitroarenes with Formic Acid. Chemistry - A European Journal, 2014, 20, 16732-16737.	1.7	42
92	Oxygen vacancy-rich, Ru-doped In <sub>2</sub> O <sub>3</sub> ultrathin nanosheets for efficient detection of xylene at low temperature. Journal of Materials Chemistry C, 2018, 6, 4156-4162.	2.7	42
93	Synthetic porous materials applied in hydrogenation reactions. Microporous and Mesoporous Materials, 2017, 237, 246-259.	2.2	40
94	Constructing Ohmic contact in cobalt selenide/Ti dyadic electrode: The third aspect to promote the oxygen evolution reaction. Nano Energy, 2017, 39, 321-327.	8.2	39
95	Mixed-bonded open-framework aluminophosphates and related layered materials. Topics in Catalysis, 1999, 9, 93-103.	1.3	38
96	General transfer hydrogenation by activating ammonia-borane over cobalt nanoparticles. RSC Advances, 2015, 5, 102736-102740.	1.7	38
97	Graphene-nanosheet-wrapped LiV3O8 nanocomposites as high performance cathode materials for rechargeable lithium-ion batteries. Journal of Power Sources, 2016, 307, 426-434.	4.0	38
98	Room-temperature spontaneous crystallization of porous amorphous titania into a high-surface-area anatase photocatalyst. Chemical Communications, 2013, 49, 8217.	2.2	37
99	Hierarchical porous carbon spheres as an anode material for lithium ion batteries. RSC Advances, 2013, 3, 10823.	1.7	36
100	A Polyimide Nanolayer as a Metalâ€Free and Durable Organic Electrode Toward Highly Efficient Oxygen Evolution. Angewandte Chemie - International Edition, 2018, 57, 12563-12566.	7.2	36
101	Germanium nanoparticles supported by 3D ordered macroporous nickel frameworks as high-performance free-standing anodes for Li-ion batteries. Chemical Engineering Journal, 2018, 354, 616-622.	6.6	36
102	Activating Oxygen Molecules over Carbonylâ€Modified Graphitic Carbon Nitride: Merging Supramolecular Oxidation with Photocatalysis in a Metalâ€Free Catalyst for Oxidative Coupling of Amines into Imines. ChemCatChem, 2016, 8, 3441-3445.	1.8	35
103	Converting waste paper to multifunctional graphene-decorated carbon paper: from trash to treasure. Journal of Materials Chemistry A, 2015, 3, 13926-13932.	5.2	34
104	Well-ordered mesoporous Fe <sub>2</sub> O <sub>3</sub> /C composites as high performance anode materials for sodium-ion batteries. Dalton Transactions, 2017, 46, 5025-5032.	1.6	34
105	Hydroquinone Resin Induced Carbon Nanotubes on Ni Foam As Binder-Free Cathode for Li–O <sub>2</sub> Batteries. ACS Applied Materials & Interfaces, 2016, 8, 3868-3873.	4.0	33
106	Two Porous Polyoxometalate-Resorcin[4]arene-Based Supramolecular Complexes: Selective Adsorption of Organic Dyes and Electrochemical Properties. Crystal Growth and Design, 2018, 18, 6046-6053.	1.4	33
107	Synthesis and X-ray crystal structures of two new alkaline-earth metal borates: SrBO2(OH) and Ba3B6O9(OH)6. Dalton Transactions RSC, 2002, , 2031-2035.	2.3	31
108	Hydrothermal synthesis and photoluminesent properties of Sb3+-doped and (Sb3+,Mn2+)-co-doped calcium hydroxyapatite. Journal of Materials Chemistry, 2002, 12, 3761-3765.	6.7	30

#	Article	IF	CITATIONS
109	Polyether-grafted SnO2 nanoparticles designed for solid polymer electrolytes with long-term stabilityElectronic supplementary information (ESI) available: XPS results and in situ IR spectra. See http://www.rsc.org/suppdata/jm/b4/b405179c/. Journal of Materials Chemistry, 2004, 14, 2775.	6.7	30
110	Nanoscale Kirkendall growth of silicalite-1 zeolite mesocrystals with controlled mesoporosity and size. Chemical Communications, 2015, 51, 12563-12566.	2.2	30
111	Ultra-durable two-electrode Zn–air secondary batteries based on bifunctional titania nanocatalysts: a Co <sup>2+</sup> dopant boosts the electrochemical activity. Journal of Materials Chemistry A, 2016, 4, 7841-7847.	5.2	30
112	The crystallinity effect of mesocrystalline BaZrO <sub>3</sub> hollow nanospheres on charge separation for photocatalysis. Chemical Communications, 2014, 50, 3021-3023.	2.2	29
113	Porous vanadium-doped titania with active hydrogen: a renewable reductant for chemoselective hydrogenation of nitroarenes under ambient conditions. Chemical Communications, 2012, 48, 9032.	2.2	28
114	Boosting Potassium Storage Capacity Based on Stressâ€Induced Sizeâ€Dependent Solidâ€Solution Behavior. Advanced Energy Materials, 2018, 8, 1802175.	10.2	28
115	Boosting the electrochemical performance of Li–O2 batteries with DPPH redox mediator and graphene-luteolin-protected lithium anode. Energy Storage Materials, 2020, 31, 373-381.	9.5	28
116	Enhanced oxygen electroreduction over nitrogen-free carbon nanotube-supported CuFeO <sub>2</sub> nanoparticles. Journal of Materials Chemistry A, 2018, 6, 4331-4336.	5.2	27
117	Isoelectric Si Heteroatoms as Electron Traps for N <sub>2</sub> Fixation and Activation. Advanced Functional Materials, 2020, 30, 2005779.	7.8	26
118	Controlled growth of Sb2O5nanoparticles and their use as polymer electrolyte fillers. Journal of Materials Chemistry, 2003, 13, 1994-1998.	6.7	25
119	Thiophene Derivative as a High Electrochemical Active Anode Material for Sodium-Ion Batteries: The Effect of Backbone Sulfur. Chemistry of Materials, 2018, 30, 8426-8430.	3.2	25
120	Effect of Surface Cations on Photoelectric Conversion Property of Nanosized Zirconia. Journal of Physical Chemistry C, 2009, 113, 9114-9120.	1.5	24
121	Cerium vanadate nanoparticles as a new anode material for lithium ion batteries. RSC Advances, 2013, 3, 7403.	1.7	24
122	Activating Pd nanoparticles on sol–gel prepared porous g-C <sub>3</sub> N <sub>4</sub> /SiO <sub>2</sub> via enlarging the Schottky barrier for efficient dehydrogenation of formic acid. Inorganic Chemistry Frontiers, 2016, 3, 1124-1129.	3.0	24
123	Freeâ€Standing Air Cathodes Based on 3D Hierarchically Porous Carbon Membranes: Kinetic Overpotential of Continuous Macropores in Liâ€O <sub>2</sub> Batteries. Angewandte Chemie, 2018, 130, 6941-6945.	1.6	24
124	Engineering the Interfaces of Superadsorbing Grapheneâ€Based Electrodes with Gas and Electrolyte to Boost Gas Evolution and Activation Reactions. ChemSusChem, 2018, 11, 2306-2309.	3.6	24
125	Free-standing N,Co-codoped TiO <sub>2</sub> nanoparticles for LiO <sub>2</sub> -based Li–O <sub>2</sub> batteries. Journal of Materials Chemistry A, 2019, 7, 23046-23054.	5.2	24
126	Electrochemical activation of C–H by electron-deficient W2C nanocrystals for simultaneous alkoxylation and hydrogen evolution. Nature Communications, 2021, 12, 3882.	5.8	24

#	Article	IF	CITATIONS
127	Programmable synthesis of mesoporous ZSM-5 nanocrystals as selective and stable catalysts for the methanol-to-propylene process. Catalysis Science and Technology, 2016, 6, 5262-5266.	2.1	23
128	Synergy of Fe-N4 and non-coordinated boron atoms for highly selective oxidation of amine into nitrile. Nano Research, 2020, 13, 2079-2084.	5.8	23
129	Sodium phthalate as an anode material for sodium ion batteries: effect of the bridging carbonyl group. Journal of Materials Chemistry A, 2020, 8, 8469-8475.	5.2	23
130	Phenoxymethylpenicillin-intercalated hydrotalcite as a bacteria inhibitor. Journal of Chemical Technology and Biotechnology, 2006, 81, 89-93.	1.6	22
131	Core–shell anatase anode materials for sodium-ion batteries: the impact of oxygen vacancies and nitrogen-doped carbon coating. Nanoscale, 2019, 11, 17860-17868.	2.8	21
132	MoS2 nanoflakes integrated in a 3D carbon framework for high-performance sodium-ion batteries. Journal of Alloys and Compounds, 2019, 797, 1126-1132.	2.8	21
133	3D ordered macroporous MoO <sub>2</sub> attached on carbonized cloth for high performance free-standing binder-free lithium–sulfur electrodes. Journal of Materials Chemistry A, 2019, 7, 24524-24531.	5.2	21
134	Dendrite-free lithium anode achieved under lean-electrolyte condition through the modification of separators with F-functionalized Ti3C2 nanosheets. Journal of Energy Chemistry, 2022, 66, 366-373.	7.1	21
135	Boosting Mass Exchange between Pd/NC and MoC/NC Dual Junctions via Electron Exchange for Cascade CO <sub>2</sub> Fixation. Journal of the American Chemical Society, 2022, 144, 5418-5423.	6.6	21
136	Chemical fixation of CO <sub>2</sub> on nanocarbons and hybrids. Journal of Materials Chemistry A, 2021, 9, 20857-20873.	5.2	20
137	Light-Driven Preparation, Microstructure, and Visible-Light Photocatalytic Property of Porous Carbon-Doped TiO <sub>2</sub> . International Journal of Photoenergy, 2012, 2012, 1-9.	1.4	19
138	Accelerated room-temperature crystallization of ultrahigh-surface-area porous anatase titania by storing photogenerated electrons. Chemical Communications, 2017, 53, 1619-1621.	2.2	19
139	The solution-phase process of a g-C <sub>3</sub> N <sub>4</sub> /BiVO <sub>4</sub> dyad to a large-area photoanode: interfacial synergy for highly efficient water oxidation. Chemical Communications, 2017, 53, 10544-10547.	2.2	19
140	Tuning the Adsorption Energy of Methanol Molecules Along Niâ€Nâ€Đoped Carbon Phase Boundaries by the Mott–Schottky Effect for Gasâ€Phase Methanol Dehydrogenation. Angewandte Chemie, 2018, 130, 2727-2731.	1.6	19
141	Oriented arrays of Co3O4 nanoneedles for highly efficient electrocatalytic water oxidation. Chemical Communications, 2019, 55, 3971-3974.	2.2	19
142	Bio-inspired noble metal-free reduction of nitroarenes using NiS <sub>2+x</sub> /g-C <sub>3</sub> N <sub>4</sub> . RSC Advances, 2014, 4, 60873-60877.	1.7	18
143	Light-Driven Transformation of ZnS-Cyclohexylamine Nanocomposite into Zinc Hydroxysulfate: A Photochemical Route to Inorganic Nanosheets. Inorganic Chemistry, 2011, 50, 9106-9113.	1.9	17
144	Single-site photocatalysts with a porous structure. Proceedings of the Royal Society A: Mathematical, Physical and Engineering Sciences, 2012, 468, 2099-2112.	1.0	16

#	Article	IF	CITATIONS
145	Synthesis and structural characterisation of a new layered aluminophosphate [C3H12N2][Al2P2O8(OH)2]·H2O. Dalton Transactions RSC, 2000, , 1981-1984.	2.3	15
146	Sensor material based on occluded trisulfur anionic radicals for convenient detection of trace amounts of water molecules. Journal of Materials Chemistry, 2010, 20, 3307.	6.7	15
147	Nonâ€Conjugated Dicarboxylate Anode Materials for Electrochemical Cells. Angewandte Chemie, 2018, 130, 9003-9008.	1.6	15
148	{M(C5H4N)CH(OH)PO3}(H2O)Â(M = Mn, Fe, Co): layered compounds based on [hydroxy(4-pyridyl)methyl]phosphonate. Dalton Transactions, 2003, , 953-956.	1.6	14
149	Monoâ€Atomic Fe Centers in Nitrogen/Carbon Monolayers for Liquidâ€Phase Selective Oxidation Reaction. ChemCatChem, 2018, 10, 3539-3545.	1.8	14
150	Synthesis of Ionic Vinyleneâ€Linked Covalent Organic Frameworks through Quaternizationâ€Activated Knoevenagel Condensation. Angewandte Chemie, 2021, 133, 13726-13732.	1.6	14
151	Facilitating Hot Electron Injection from Graphene to Semiconductor by Rectifying Contact for Vis–NIRâ€Đriven H <sub>2</sub> O <sub>2</sub> Production. Small, 2022, 18, e2200885.	5.2	14
152	Synthesis, structures and photoluminescence of two Er(III) coordination polymers. Journal of Coordination Chemistry, 2008, 61, 945-955.	0.8	13
153	Chemical "top-down―synthesis of amphiphilic superparamagnetic Fe <sub>3</sub> O <sub>4</sub> nanobelts from exfoliated FeOCl layers. Dalton Transactions, 2014, 43, 16173-16177.	1.6	13
154	In situ growth of ultrafine tin oxide nanocrystals embedded in graphitized carbon nanosheets for use in high-performance lithium-ion batteries. Journal of Materials Chemistry A, 2014, 2, 6960-6965.	5.2	13
155	Uric Acid as an Electrochemically Active Compound for Sodium-Ion Batteries: Stepwise Na <sup>+</sup> -Storage Mechanisms of i€-Conjugation and Stabilized Carbon Anion. ACS Applied Materials & Interfaces, 2017, 9, 33934-33940.	4.0	13
156	Atomically Dispersed Ni-Based Anti-Coking Catalysts for Methanol Dehydrogenation in a Fixed-Bed Reactor. ACS Catalysis, 2020, 10, 12569-12574.	5.5	13
157	Schottky Barrierâ€Induced Surface Electric Field Boosts Universal Reduction of NO x â^' in Water to Ammonia. Angewandte Chemie, 2021, 133, 20879-20884.	1.6	12
158	Rubber-based carbon electrode materials derived from dumped tires for efficient sodium-ion storage. Dalton Transactions, 2018, 47, 4885-4892.	1.6	11
159	Autoxidation of polythiophene tethered to carbon cloth boosts its electrocatalytic activity towards durable water oxidation. Journal of Materials Chemistry A, 2020, 8, 19793-19798.	5.2	11
160	Synthesis, structure and photoluminescence of two zinc carboxylate polymers with different coordination architectures. Chinese Journal of Chemistry, 2003, 21, 1305-1308.	2.6	10
161	Transitions from a Kondo-like diamagnetic insulator into a modulated ferromagnetic metal in FeGa <sub>3â^'y</sub> Ge <sub>y</sub> . Proceedings of the National Academy of Sciences of the United States of America, 2018, 115, 3273-3278.	3.3	10
162	Phosphazene-derived stable and robust artificial SEI for protecting lithium anodes of Li–O <sub>2</sub> batteries. Chemical Communications, 2020, 56, 12566-12569.	2.2	10

#	Article	IF	CITATIONS
163	Thiophene derivatives as electrode materials for high-performance sodium-ion batteries. Journal of Materials Chemistry A, 2021, 9, 11530-11536.	5.2	10
164	Heteroatomâ€Embedded Approach to Vinyleneâ€Linked Covalent Organic Frameworks with Isoelectronic Structures for Photoredox Catalysis. Angewandte Chemie, 2022, 134, e202111627.	1.6	10
165	A Polyimide Nanolayer as a Metalâ€Free and Durable Organic Electrode Toward Highly Efficient Oxygen Evolution. Angewandte Chemie, 2018, 130, 12743-12746.	1.6	9
166	Photogenerated singlet oxygen over zeolite-confined carbon dots for shape selective catalysis. Science China Chemistry, 2019, 62, 434-439.	4.2	9
167	Biomimetic Design of a 3 D Transition Metal/Carbon Dyad for the One‣tep Hydrodeoxygenation of Vanillin. ChemSusChem, 2020, 13, 1900-1905.	3.6	9
168	Distinct effect of hierarchical structure on performance of anatase as an anode material for lithium-ion batteries. RSC Advances, 2013, 3, 26052.	1.7	8
169	Trapping oxygen in hierarchically porous carbon nano-nets: graphitic nitrogen dopants boost the electrocatalytic activity. RSC Advances, 2016, 6, 56765-56771.	1.7	8
170	Mesoporous <scp>TS</scp> â€I Nanocrystals as Low Cost and High Performance Catalysts for Epoxidation of Styrene. Chinese Journal of Chemistry, 2017, 35, 577-580.	2.6	8
171	Designed electron-deficient gold nanoparticles for a room-temperature Csp3–Csp3 coupling reaction. Chemical Communications, 2021, 57, 741-744.	2.2	8
172	Oxygen Vacancy Engineering of Titania-Induced by Sr2+ Dopants for Visible-Light-Driven Hydrogen Evolution. Inorganic Chemistry, 2021, 60, 32-36.	1.9	8
173	Eu3+and Lysine Co-intercalated Â-Zirconium Phosphate and Its Catalytic Activity for Copolymerization of Propylene Oxide and CO2. Catalysis Letters, 2004, 94, 95-102.	1.4	7
174	Grouping Effect of Single Nickelâ^'N 4 Sites in Nitrogenâ€Doped Carbon Boosts Hydrogen Transfer Coupling of Alcohols and Amines. Angewandte Chemie, 2018, 130, 15414-15418.	1.6	7
175	Synergy of B and Al Dopants in Mesoporous MFI Nanocrystals for Highly Selective Alcoholysis of Furfuryl Alcohol into Ethyl Levulinate. Energy Technology, 2019, 7, 1900271.	1.8	7
176	Heterojunctionâ€Based Electron Donators to Stabilize and Activate Ultrafine Pt Nanoparticles for Efficient Hydrogen Atom Dissociation and Gas Evolution. Angewandte Chemie, 2021, 133, 25970-25974.	1.6	7
177	A Polyimide-Based Photocatalyst for Continuous Hydrogen Peroxide Production Using Air and Water under Solar Light. CCS Chemistry, 2022, 4, 3482-3490.	4.6	7
178	Construction of Large Nonâ€Localized Ï€â€Electron System for Enhanced Sodiumâ€Ion Storage. Small, 2022, 18, e2105825.	5.2	7
179	Supramolecular nano-assemblies with tailorable surfaces: recyclable hard templates for engineering hollow nanocatalysts. Science China Materials, 2014, 57, 7-12.	3.5	6
180	Preparation of Porous Silicon by Sodiothermic Reduction of Zeolite and Photoactivation for Benzene Oxidation. European Journal of Inorganic Chemistry, 2015, 2015, 1330-1333.	1.0	6

#	Article	IF	CITATIONS
181	Direct reduction of oxygen gas over dendritic carbons with hierarchical porosity: beyond the diffusion limitation. Inorganic Chemistry Frontiers, 2018, 5, 2023-2030.	3.0	6
182	Towards high performance lithium-oxygen batteries: Co3O4-NiO heterostructure induced preferential growth of ultrathin Li2O2 film. Journal of Alloys and Compounds, 2021, 863, 158073.	2.8	6
183	Experimental Validation of the Importance of Thermally Stable Bulk Reduction States in TiO <sub>2</sub> for Gas Sensor Applications. Acta Chimica Sinica, 2012, 70, 1477.	0.5	6
184	Use of Nitrogen-Containing Carbon Supports To Control the Acidity of Supported Heteropolyacid Model Catalysts. Industrial & Engineering Chemistry Research, 2018, 57, 13999-14010.	1.8	5
185	Accelerating the Activation of NO <sub>x</sub> <sup>â^²</sup> on Ru Nanoparticles for Ammonia Production by Tuning Their Electron Deficiency. CCS Chemistry, 2022, 4, 3455-3462.	4.6	5
186	Synthesis and Characterization of Ethylenediammonium Molybdenum Thiocomplex [H <sub>3</sub> NCH <sub>2</sub> CH <sub>2</sub> NH <sub>3</sub> ][Mo <sub>3</sub> S <sub>13</sub> ]. Chinese Journal of Chemistry, 2001, 19, 681-688.	2.6	4
187	Formation of a built-in field at the porphyrin/ITO interface directly proven by the time-resolved photovoltage technique. Physical Chemistry Chemical Physics, 2015, 17, 5202-5206.	1.3	4
188	Top-down fabrication of hierarchical nanocubes on nanosheets composite for high-rate lithium storage. Dalton Transactions, 2018, 47, 16155-16163.	1.6	4
189	Enhanced Electrochemical Performance of Aprotic Li O <sub>2</sub> Batteries with a Ruthenium omplexâ€Based Mobile Catalyst. Angewandte Chemie, 2021, 133, 16540-16544.	1.6	4
190	Roomâ€Temperature Activation of Molecular Oxygen Over a Metalâ€Free Triazineâ€Decorated sp <sup>2</sup> â€Carbon Framework for Green Synthesis. ChemCatChem, 2018, 10, 5331-5335.	1.8	3
191	(Ć <sub>14</sub> N <sub>14</sub> H <sub>63</sub> ) (H <sub>2</sub> Mo <sub>6</sub> P <sub>4</sub> O <sub>31</sub> ) <sub>2</sub> · 8H <sub>2</sub> O and (C <sub>14</sub> N <sub>14</sub> H <sub>64</sub> 0 <sub>31</sub> ) <sub>22</sub> · 5H <sub>22</sub> 0 (H <sub>22</sub> 22	2.6	2
192	Chinese Journal of Chemistry, 2002, 20, 858-864. Facile preparation and cellular imaging of photoluminescent carbogenic nanoparticles derived from defoliations. Chemical Research in Chinese Universities, 2013, 29, 189-192.	1.3	1
193	Semiconductorâ€based nanocomposites for selective organic synthesis. Nano Select, 2021, 2, 1799.	1.9	1
194	Tunable Surface Electric Field of Electrocatalysts via Constructing Schottky Heterojunctions for Selective Conversion of Trash lons to Treasures. Chemistry - A European Journal, 2022, 28, .	1.7	1
195	Frontispiece: Tunable Surface Electric Field of Electrocatalysts via Constructing Schottky Heterojunctions for Selective Conversion of Trash Ions to Treasures. Chemistry - A European Journal, 2022, 28, .	1.7	1
196	Formation of nanographite using GaPO <sub>4</sub> ‣TA as template. Chinese Journal of Chemistry, 2004, 22, 1399-1402.	2.6	0
197	Back Cover: Efficient Sunlight-Driven Dehydrogenative Coupling of Methane to Ethane over a Zn+-Modified Zeolite (Angew. Chem. Int. Ed. 36/2011). Angewandte Chemie - International Edition, 2011, 50, n/a-n/a.	7.2	0
198	Materials Research at Shanghai Jiao Tong University. Advanced Materials, 2015, 27, 400-402.	11.1	0

1	UAN	CII
J	UAN	Ju

#	Article	IF	CITATIONS
199	SYNTHESIS AND X-RAY CRYSTAL STRUCTURES OF LOW-DIMENSIONAL BORATES FROM HYDROTHERMAL AND SOLVOTHERMAL SYSTEMS. , 2002, , .		Ο